

# Order and disorder at the C-face of SiC: A hybrid surface reconstruction

Cite as: Appl. Phys. Lett. **116**, 141605 (2020); <https://doi.org/10.1063/1.5143010>

Submitted: 18 December 2019 . Accepted: 23 March 2020 . Published Online: 09 April 2020

Eduardo Machado-Charry , César González , Yannick J. Dappe , Laurence Magaud , Normand Mousseau , and Pascal Pochet 



View Online



Export Citation



CrossMark



## Instruments for Advanced Science

Contact Hiden Analytical for further details:

**W** [www.HidenAnalytical.com](http://www.HidenAnalytical.com)

**E** [info@hiden.co.uk](mailto:info@hiden.co.uk)

**CLICK TO VIEW** our product catalogue

**Gas Analysis**

- dynamic measurement of reaction gas streams
- catalysis and thermal analysis
- molecular beam studies
- dissolved species probes
- fermentation, environmental and ecological studies

**Surface Science**

- UHV/TPO
- SIMS
- end point detection in ion beam etch
- elemental imaging - surface mapping

**Plasma Diagnostics**

- plasma source characterization
- etch and deposition process reaction kinetic studies
- analysis of neutral and radical species

**Vacuum Analysis**

- partial pressure measurement and control of process gases
- reactive sputter process control
- vacuum diagnostics
- vacuum coating process monitoring

# Order and disorder at the C-face of SiC: A hybrid surface reconstruction

Cite as: Appl. Phys. Lett. **116**, 141605 (2020); doi: [10.1063/1.5143010](https://doi.org/10.1063/1.5143010)

Submitted: 18 December 2019 · Accepted: 23 March 2020 ·

Published Online: 9 April 2020



View Online



Export Citation



CrossMark

Eduardo Machado-Charry,<sup>1</sup> César González,<sup>2</sup> Yannick J. Dappe,<sup>3</sup> Laurence Magaud,<sup>4</sup> Normand Mousseau,<sup>5</sup> and Pascal Pochet<sup>6,a)</sup>

## AFFILIATIONS

<sup>1</sup>Institute of Solid State Physics and NAWI Graz, Graz University of Technology, Petersgasse 16, 8010 Graz, Austria

<sup>2</sup>Departamento de Física Teórica de la Materia Condensada and Condensed Matter Physics Center, Facultad de Ciencias, Universidad Autónoma de Madrid, E-28049 Madrid, Spain

<sup>3</sup>SPEC, CEA, CNRS, Université Paris-Saclay, CEA Saclay, 91191 Gif-sur-Yvette Cedex, France

<sup>4</sup>Univ. Grenoble Alpes, CNRS, Institut Neel, F-38042 Grenoble, France

<sup>5</sup>Département de physique and RQMP, Université de Montréal, Case Postale 6128, Succursale Centre-ville, Montréal, Québec H3C 3J7, Canada

<sup>6</sup>Department of Physics, IriG, Univ. Grenoble Alpes and CEA, F-38000 Grenoble, France

<sup>a)</sup> Author to whom correspondence should be addressed: [pascal.pochet@cea.fr](mailto:pascal.pochet@cea.fr)

## ABSTRACT

In this Letter, we explore the potential energy surface (PES) of the  $3 \times 3$  C-face of SiC by means of the density functional theory. Following an extensive and intuitive exploration, we propose a model for this surface reconstruction based on an all-silicon over-layer forming an ordered honeycomb-Kagome network. This model is compared to the available scanning tunneling microscope (STM) topographies and conductance maps. Our STM simulations reproduce the three main characteristics observed in the measurements, revealing the underlying complex and hybrid passivation scheme. Indeed, below the ordered over-layer, the competition between two incompatible properties of silicon induces a strong disorder in the charge transfer between unpassivated dangling bonds of different chemistry. This effect in conjunction with the glassy-like character of the PES explains why it has taken decades to provide an accurate atomistic representation for this structure.

Published under license by AIP Publishing. <https://doi.org/10.1063/1.5143010>

Semiconductor surfaces reconstruct mainly through the insertion of ad-atoms or through self-reorganization.<sup>1</sup> In the former case, dangling bonds are passivated as bonds are created with additional atoms; in the latter, dangling bonds are partially or completely eliminated via some charge transfer. Although reconstruction usually follows one of these two schemes, both mechanisms are sometimes mixed. This hybrid mechanism generally occurs when some unpassivated surface atoms (known as *rest atoms*<sup>1</sup>) undergo a charge transfer with the ad-atoms and lead to a surface that exhibits both a commensurate and ordered super-structure. A deep understanding of these reconstruction mechanisms is central to applied physics, particularly for growth science, as well as for tuning devices that make use of interfacial physics such as 2D electron gas and surface superconductivity.<sup>2</sup>

In spite of its technological importance for the growth of graphene from hexagonal SiC (*H*-SiC), a surface reconstruction at the carbon face (000 $\bar{1}$ ) has remained unresolved for more than two decades. We show in the following that this reconstruction (known as

$3 \times 3$ ) corresponds to a hybrid reconstruction, in which an ordered network of ad-atoms and a partial intermixing at the level of the rest-atoms lead to an unusually incommensurate yet ordered structure.

The  $3 \times 3$  reconstruction was first imaged by means of scanning tunneling microscopy (STM) in 1997.<sup>3</sup> This system shows a clear distinction between STM features at occupied states ( $stm_o$ ) and unoccupied states ( $stm_u$ ). Several attempts<sup>3–7</sup> to explain these observations with an atomic model of the surface were unsuccessful, in part because the exact composition of the surface as well as the affected number of layers cannot be obtained from the experimental data. The difficulty of determining the composition of the bare  $3 \times 3$  reconstruction is increased as this surface evolves as the temperature is raised, leading to the formation of the surface graphene layer.<sup>8</sup> In 2012, cutting-edge STM data<sup>5,9</sup> revealed unique features for the  $3 \times 3$  surface at an energy range close to zero bias ( $stm_g$ ). The three experimental STM images are reproduced in Figs. 1(a)–1(c). Following the notation in Ref. 3, the different features are described in terms of three symmetry points

of the surface cell, namely  $A$ ,  $B$ , and  $C$  positioned at  $(\frac{1}{3}, \frac{1}{3})$ ,  $(\frac{2}{3}, \frac{2}{3})$ , and  $(1, 1)$ , respectively. The  $stm_o$  image shows a simple kagome-like pattern where sites  $A$  and  $B$ , at the center of each triangle, have the same intensity and are equivalent by rotation. The equivalence is broken at  $stm_u$  image where a clear wide spot is visible in the surface cell only at site  $A$ . For their part, sites  $C$  show low intensity values in both  $stm_o$  and  $stm_u$  images. The overall picture is quite different at a low bias, i.e.,  $stm_g$  image [Fig. 1(c)], where only signals from some  $C$  sites are observed when analyzing the conductance images of several adjacent surface cells; notably, bright and dark signals at  $C$  sites (labeled  $C^+$  and  $C^-$ ) appear without any clear order. The analysis of different images shows that the  $C^+$  sites represent between 60% and 70% of the total number of  $C$  sites.<sup>5</sup>

This puzzling situation has motivated us to explore the potential energy surface (PES) for this system in order to identify the structure. An exhaustive search for the PES, with methods such as the activation-relaxation technique<sup>10</sup> is, however, not possible today. The main reason is that both silicon and carbon easily form complex structures, thus the PES of the SiC surface is complex, almost glassy-like in character.<sup>11</sup> This suggests that a complete exploration of the landscape would require sampling a large number of states, many accessible only through highly non-equilibrium pathways.

We chose to pursue an extensive manual search mainly driven by user intuition and comparison spanning over a large range of surface concentration as depicted in Fig. 2(a), see the details below.

Energy optimization for all considered configurations is determined using BigDFT with surface conditions<sup>12</sup> in a  $3 \times 3$  orthorhombic cell containing four SiC bilayers stacked in  $4H$ , with the silicon atoms of the bottom bilayer being hydrogen passivated. The local-density approximation functional and 2 k-points in the zigzag direction are used in addition to the standard parameters.<sup>10</sup> For the surface formation energy (FE), we assume thermodynamic equilibrium with respect to the bulk  $4H$ -SiC, white window in Fig. 2(c). In this window,  $\mu_C + \mu_{Si} = E_{SiC}^{bulk}$ , where  $\mu_C$  and  $\mu_{Si}$  are the chemical potentials for C and Si, respectively, and  $E_{SiC}^{bulk}$  is the total energy of the bulk  $4H$ -SiC unit cell.<sup>6</sup> Based on the FE plot, selected configurations (see below) are further analyzed with the Fireball package.<sup>13</sup> Hence, partial DOS are extracted, and combined with a realistic  $W$  tip to simulate the corresponding STM images.<sup>14</sup>

In 2015, while analyzing high-quality STM topographies for the ultra-thin silicon dioxide layer grown on  $2 \times 2$  Ru oxide,<sup>15</sup> we identified some similarities between the two systems. Figures 1(a) and 1(d) show that there is a clear correspondence between the  $stm_o$  image of the  $3 \times 3$  reconstruction and the STM image of the silica ad-layer on Ru oxide. Both show a Kagome network, the only difference being that the  $C$  site is always bright in the latter. Although both images were taken at different polarities, the known configuration of the silica ( $Si_2O_3$ ) on Ru oxide [Figs. 1(e) and 1(f)] is used as a template for the  $3 \times 3$  reconstruction. Thus, we can simply *transmute* each bridging oxygen of the silica into a bridging silicon atom. This results in an almost flat over-layer made of five silicon ad-atoms [Figs. 1(g) and 1(h)]. Due to its two dimensional character, this layered model is called  $2DL_1$  in our exploration nomenclature [Fig. 2(b)]. This model was recently and independently proposed as a possible candidate for the  $3 \times 3$  although no STM simulation was reported.<sup>16</sup>

As can be seen in Figs. 1(i) and 1(j), the simulated STM images based on the  $2DL_1$  model nicely reproduce both experimental  $stm_o$

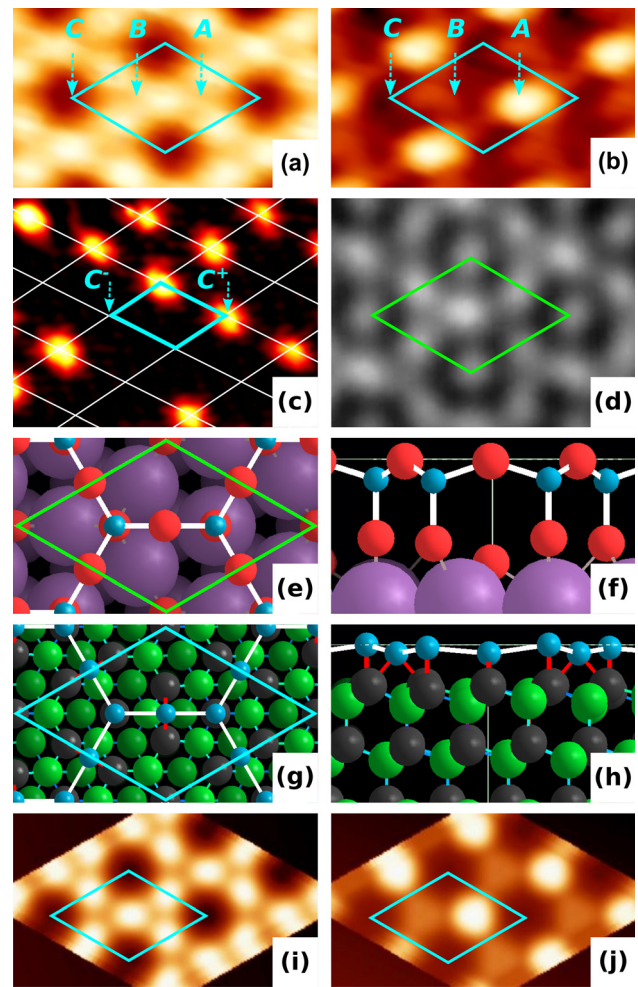


**FIG. 1.** The SiC  $3 \times 3$  (cyan rhombus) reconstruction. STM at different voltages [Reproduced with permission from F. Hiebel, "Investigation of the graphene—SiC(000-1) (carbon face) interface using scanning tunneling microscopy and ab initio numerical simulations," Ph.D. thesis (University Grenoble Alpes, 2011)<sup>4</sup>]: (a)  $stm_o$  at  $-2.5$  V, (b)  $stm_u$  at  $2.5$  V, and (c)  $stm_g$  at  $-0.65$  V. (d) STM of ultra-thin silica on  $2 \times 2$  (green rhombus) Ru oxide measured at  $0.9$  V [Reproduced with permission from S. Mathur, "Growth and atomic structure of a novel crystalline two-dimensional material based on silicon and oxygen," Ph.D. thesis (University Grenoble Alpes, 2016)<sup>21</sup>]. (e) and (f) This film is composed of two Si ad-atoms, respectively, on the top and hollow Ru positions<sup>15</sup> and three bridging O atoms (defining O sites). Si, O, and Ru atoms are blue, red, and purple, respectively. The  $2DL_1$  model (g) and (h) contains 2 top Si ad-atoms on A and B sites and three bridging Si on O sites. These five ad-atoms forming an over-layer are shown in blue and their connections with the carbon dangling bonds are represented by red bonds, whereas bulk Si and C atoms are green and black. STM simulations of  $2DL_1$  at  $-2.5$  V (i) and  $+2.5$  V (j) to be compared to (a) and (b), respectively.

and  $stm_u$  images. Through careful scrutiny of these images, symmetry sites  $A$  and  $B$  in Figs. 1(a) and 1(b) can be identified with the two non-bridging silicon atoms, i.e., with the two silicon atoms of the silica model forming a honeycomb network. On the other hand, the three bridging silicon atoms are responsible for the bright STM features in the Kagome pattern, as the bridging O atoms do for silica [Fig. 1(d)].

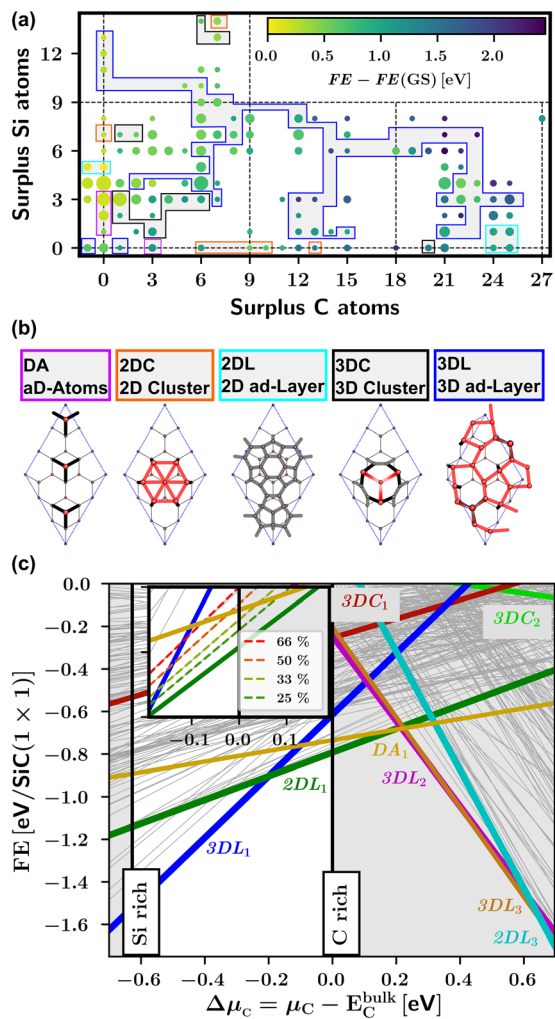


**FIG. 2.** The intensive PES exploration of the  $3 \times 3$  SiC surface. (a) Scatter plot of the evaluated models as a function of the surplus at the surface of C and Si atoms with respect to the raw bulk-terminated  $3 \times 3$  surface. The radius of each circle is proportional to the number of considered models at a given surface chemistry. The dotted lines correspond to a full addition/removal of atoms of the same type in the last SiC bilayer. Closed contours correspond to sectors of a given topology class for the lowest FE model at each concentration point. Color is scaled on formation energy at  $\Delta\mu_C = 0$  in reference to the lowest energy model, i.e., the  $2DL_1$  one at  $(C=0, Si=5)$ . (b) A schematic view of examples for the five class of topologies: pure ad-atoms, 2D and 3D cluster of ad-atoms, and 2D and 3D ad-layers covering the whole surface. Si and C atoms are in red and gray, respectively. (c) Surface formation energy as a function of the carbon chemical potential. FE was calculated relative to the raw bulk-terminated  $(1 \times 1)$  4H-SiC surface. The SiC bulk is stable in the range  $-0.628 \leq \mu_C - E_C^{\text{bulk}} \leq 0$  eV. Some previous models are:  $3DL_1$  (blue),<sup>6</sup>  $3DC_2$  (lime green),<sup>7</sup> and  $3DC_1$  (dark red).<sup>3</sup>

We will refer to these bridging sites as *O* sites in the following. Thus, silicon ad-atoms at sites *A*, *B*, and *O* form a honeycomb-Kagome network.

The  $2DL_1$  over-layer, despite the previous results, fails to reproduce the third STM condition, i.e., the  $stm_g$  image. This discrepancy is a weak but clear signal that something is still missing in this atomic

model of the surface. Indeed, in addition to the three previously discussed STM conditions, the model structure must also display a low formation energy FE to be a reasonable candidate. Meeting these four constraints in a single model is a challenge as demonstrated by previously published models,<sup>3–7</sup> that also have failed to reproduce one or the other conditions.

To face this challenge, it is necessary to gain a deeper insight regarding the nature of the energy landscape through the exploration and characterization of a wide range of possible configurations. Figure 2(c) depicts the grand potential energy for some of the 700 models (gray lines) considered in our study, demonstrating the potential richness of this surface. These models were constructed by exploring a broad range of surface concentrations starting from known surface reconstructions of similar topology.<sup>3,4,7,17</sup> Each model represents a modification in the stoichiometry of the latter but preserves the  $3 \times 3$  symmetry. The distribution of the considered surface concentration is depicted Fig. 2(a), where the radius of each circle is proportional to the number of considered models at a given surface chemistry. We classify our models into five major class that are sketched in Fig. 2(b). The colored lines in Fig. 2(c) highlight the models with the lower formation energy in a given chemical potential window. These lower bound models fulfill by definition the FE condition. In particular, the  $2DL_1$  model shows the lowest found FE at  $\mu_C - E_C^{\text{bulk}} = 0$ , where it is also close in energy with the  $(2 \times 2)_C$  phase (model  $DA_1$  in the plot).<sup>18</sup> Interestingly, the latter was observed in coexistence with the  $3 \times 3$  in a ultrahigh vacuum around  $1075^\circ\text{C}$ .<sup>19</sup>

We also colorize the three significant models of the literature that claim to reproduce the  $3 \times 3$  reconstruction but failed either for thermodynamics reasons<sup>3,7</sup> or STM incompatibility.<sup>6</sup> The model proposed by Nemeč *et al.*<sup>6</sup> [ $3DL_1$  in Fig. 2(c)] is interesting as it was the first to be a pure silicon structure that turns out to have a large stability range compatible with that of the SiC bulk.

In order to understand why the  $2DL_1$  silicon over-layer does not reproduce the  $stm_g$  image, it is necessary to analyze the interaction of this layer with the last carbon layer. Among the nine dangling bonds in the  $3 \times 3$  cell, two are passivated by the silicon ad-atoms in the top position (*A* and *B* sites), six are passivated by the three bridging Si connecting (*O* sites), while the last dangling bond (*C* site) remains non passivated. These type of atoms present a large peak in the DOS at the Fermi level (not shown) associated with their half-filled dangling-bonds.

Pursuing along with our analogy with the silica over-layer for which we recently got more insight,<sup>20</sup> we build a supercell of the  $2DL_1$  where some of the carbon atoms at the *C* site are substituted by silicon atoms. The calculations are done in a  $9 \times 6$  orthorhombic supercell containing 12 *C* sites that allow substitutions ranging from 25 to 66%. The formation energy for different ratios of silicon substitutions is depicted in the inset of Fig. 2(c); from a thermodynamic point of view, these substitutions at the *C* site are less stable than the parent  $2DL_1$  and thus can be viewed as defective.

In order to observe the effect of these substitutions on the STM images at energies close to zero bias, we use a smaller supercell, because we find that the contrast in the simulated images is quite sensitive to the thickness of the slab. Therefore, in a  $3 \times 3$  orthorhombic supercell with twice the thickness of our original 4H-SiC slab, we recalculate a model with 50% of substitution. Thus, the model contains only two inequivalent *C* sites [Fig. 3(d)]. The corresponding STM

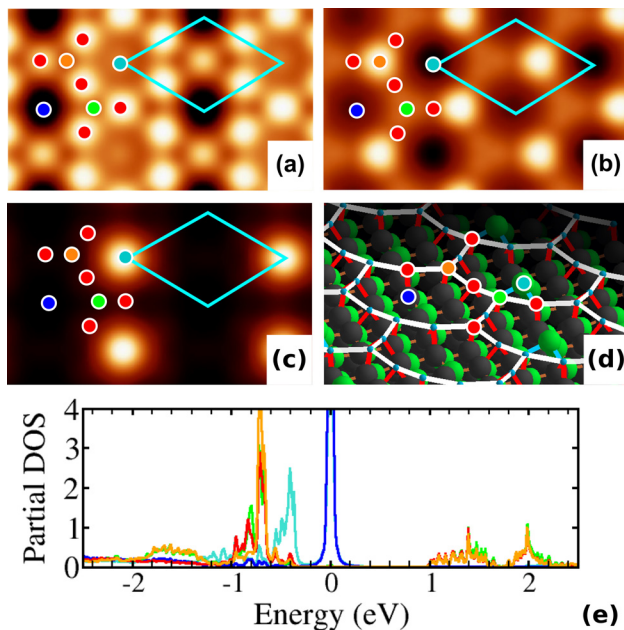


**FIG. 3.** STM images of a  $2DL_1$  supercell with 50% silicon substituted C sites at different voltages: (a)  $-2.5$  V, (b)  $2.5$  V, and (c)  $-0.45$  V. The five different site types are marked by colored circles: A (orange), B (green),  $C^+$  (light blue),  $C^-$  (dark blue), and O sites (red). The surface cell of the  $3 \times 3$  is represented by a cyan rhombus. (d) 3D view of the surface with the color marks used in a-c panels. (e) The partial DOS for the five type of atoms highlighted in (d). Color lines follow the same color code as in (d).

simulations are depicted in Figs. 3(a)–3(c) together with the partial DOS for the surface atoms lying at the four characteristic sites A, B, C, and O in panel (e).

In the partial DOS, we observe a change in the charge transfer on one hand between the carbon atom and the silicon atom at both C sites, and, on the other hand, between both atoms at C sites and the silicon over-layer. Interestingly, a state appears below the Fermi level [light blue in Fig. 3(d)] due to the silicon atom substituting one of the carbon atom at the C site. The energy range of this silicon state is broad (almost 0.3 eV) and centered around  $-0.45$  eV. More precisely, this  $-0.45$  eV state corresponds to  $p_x$  and  $p_y$  orbitals hybridized with the three neighboring silicon atoms, on the last SiC bilayer, whereas the state at the Fermi level is of  $s$  and  $p_z$  character. The simulated STM image at  $-0.45$  V [Fig. 3(c)] clearly allows to assign this silicon defect at the C site as the  $C^+$  defect observed by Hiebel *et al.*<sup>5,9</sup> Subsequently, the  $C^-$  sites are ascribed to the last carbon atom presenting a dangling bond in the parent  $2DL_1$  model. Interestingly, the carbon atoms at the  $C^-$  sites are drawn toward the surface whereas silicon atoms at the  $C^+$  sites relax outward [Fig. 3(d)] with a height difference of  $0.5 \text{ \AA}$  between both sites. This height difference is consistent with the differences observed in the profile lines from the STM images [ $\approx 0.4$  and  $0.5 \text{ \AA}$  in Fig. 1(c) in Ref. 5] further confirming the present assignment of  $C^+$  and  $C^-$  sites. This small difference, moreover, has an impact in the low intensity values of these sites in the simulated STM image at  $-2.5$  V [Fig. 3(a)]. This is also confirmed by the experimental topographies [Fig. 1(b) of Ref. 5].

Finally, the disorder seems to derive from the complex charge transfer between  $C^+$  and  $C^-$  sites and the over-layer. In order to introduce the idea of disorder, we have to acknowledge that the charge transfer is incomplete as some electrons stay on  $C^-$  sites, leading to the peak at the Fermi level. We suspect that this partial charge transfer comes from a competition between the two following properties: a larger bond length for Si–Si with respect to C–Si and a lower electronegativity for silicon with respect to carbon. Indeed, the first property would drive Si-substituted C sites to a  $C^+$  topology, while the second would drive them to the  $C^-$  topology. This competition leads the whole system to an incommensurate charge transfer in the supercell with the two C sites. This analysis is consistent with the experimental ratio of  $C^+$  sites being  $\approx 65\%$ , as indeed a 50% ratio would correspond to a full and commensurate charge transfer. The occurrence of such a disorder at C sites in the experimental STM [Fig. 1(c)] is an additional proof that a perfect passivation coming from complete charge transfer can not be found in a finite size supercell. This is an important point for graphene growth as this over-layer is interfaced with graphene.

In summary, based on an extensive exploration of the surface PES, we propose an energetically favorable atomic model that reproduces the three main STM conditions reported for the  $3 \times 3$  reconstruction of the C-face of SiC.<sup>5</sup> This model is close to that of the silica over-layer grown on Ru oxide.<sup>15</sup> It forms an all-silicon honeycomb-kagome network at the surface of a  $3 \times 3$  supercell that passivates 8 out of the 9 carbon dangling bonds in the supercell. The last carbon dangling bond is passivated through a charge transfer between Si-substituted and un-substituted sites. This charge transfer is, however, not commensurate with the lattice due to a competition between the bond length and the electronegativity of silicon with respect to carbon. This competition explains the disordered character at the level of C sites. In other words, the system has a hybrid reconstruction with an ordered network of ad-atoms and a partial intermixing at the level of C sites. This leads to a hybrid incommensurate and ordered structure.

E.M.C., L.M., N.M., and P.P. acknowledge the financial support from the NanoScience Foundation (MUSCADE project). N.M. also acknowledges the financial support from the Natural Sciences and Engineering Research Council of Canada. C.G. acknowledges the financial support by the Spanish government through Project No. MAT2017-88258-R and the “María de Maeztu” Program for Units of Excellence in R&D (No. CEX2018-000805-M). The BigDFT calculations were done using French supercomputers (GENCI) through Project No. 6194 and the supercomputers of Calcul Québec/Compute Canada. E.M.C. and P.P. acknowledge the stimulating discussions with Dr. Fanny Hiebel, Dr. Jean-Yves Veullen, and Dr. Pierre Mallet and their valuable collaboration.

## REFERENCES

- G. P. Srivastava, *Rep. Prog. Phys.* **60**, 561 (1997).
- C. Brun, T. Cren, and D. Roditchev, *Superconductor Sci. Technol.* **30**, 013003 (2017).
- H. E. Hoster, M. A. Kulakov, and B. Bullemer, *Surf. Sci.* **382**, L658 (1997).
- L. Li and I. S. T. Tsong, *Surf. Sci.* **351**, 141 (1996).
- F. Hiebel, L. Magaud, P. Mallet, and J.-Y. Veullen, *J. Phys. D: Appl. Phys.* **45**, 154003 (2012).

- <sup>6</sup>L. Nemeč, F. Lazarević, P. Rinke, M. Scheffler, and V. Blum, *Phys. Rev. B* **91**, 161408(R) (2015).
- <sup>7</sup>I. Deretzis and A. La Magna, *Appl. Phys. Lett.* **102**, 093101 (2013).
- <sup>8</sup>F. Hiebel, P. Mallet, F. Varchon, L. Magaud, and J.-Y. Veuillen, *Solid State Commun.* **149**, 1157 (2009).
- <sup>9</sup>F. Hiebel, “Investigation of the graphene—SiC(000-1) (carbon face) interface using scanning tunneling microscopy and ab initio numerical simulations,” Ph.D. thesis (University Grenoble Alpes, 2011); available at <https://tel.archives-ouvertes.fr/tel-00680068v1>.
- <sup>10</sup>E. Machado-Charry, L. K. Béliand, D. Caliste, L. Genovese, T. Deutsch, N. Mousseau, and P. Pochet, *J. Chem. Phys.* **135**, 034102 (2011).
- <sup>11</sup>S. De, A. Willand, M. Amsler, P. Pochet, L. Genovese, and S. Goedecker, *Phys. Rev. Lett.* **106**, 225502 (2011).
- <sup>12</sup>L. Genovese, A. Neelov, S. Goedecker, T. Deutsch, S. A. Ghasemi, A. Willand, D. Caliste, O. Zilberberg, M. Rayson, A. Bergman, and R. Schneider, *J. Chem. Phys.* **129**, 014109 (2008).
- <sup>13</sup>J. P. Lewis, P. Jelínek, J. Ortega, A. A. Demkov, D. G. Trabada, B. Haycock, H. Wang, G. Adams, J. K. Tomfohr, E. Abad, H. Wang, and D. A. Drabold, *Phys. Status Solidi B* **248**, 1989–2007 (2011).
- <sup>14</sup>C. González, E. Abad, Y. J. Dappe, and J. C. Cuevas, *Nanotechnology* **27**, 105201 (2016).
- <sup>15</sup>S. Mathur, S. Vlačić, E. Machado-Charry, A.-D. Vu, V. Guisnet, P. David, E. Hadji, P. Pochet, and J. Coraux, *Phys. Rev. B* **92**, 161410(R) (2015).
- <sup>16</sup>J. Li, Q. Wang, G. He, M. Widom, L. Nemeč, V. Blum, M. Kim, P. Rinke, and R. M. Feenstra, *Phys. Rev. Mater.* **3**, 084006 (2019).
- <sup>17</sup>N. Srivastava, G. He, Luxmi, and R. M. Feenstra, *Phys. Rev. B* **85**, 041404(R) (2012).
- <sup>18</sup>L. Magaud, F. Hiebel, F. Varchon, P. Mallet, and J.-Y. Veuillen, *Phys. Rev. B* **79**, 161405(R) (2009).
- <sup>19</sup>J. Hass, W. A. de Heer, and E. H. Conrad, *J. Phys.: Condens. Matter* **20**, 323202 (2008).
- <sup>20</sup>G. Kremer, J. C. Alvarez Quiceno, S. Lisi, T. Pierron, C. González, M. Sicot, B. Kierren, D. Malterre, J. E. Rault, P. Le Fèvre, F. Bertran, Y. J. Dappe, J. Coraux, P. Pochet, and Y. Fagot-Revurat, *ACS Nano* **13**, 4720 (2019).
- <sup>21</sup>S. Mathur, “Growth and atomic structure of a novel crystalline two-dimensional material based on silicon and oxygen,” Ph.D. thesis (University Grenoble Alpes, 2016); available at <https://tel.archives-ouvertes.fr/tel-01486932v2>.